Peer-reviewed version available at Coatings 2019, 9, 279; doi:10.3390/coatings9040279

Article

Electrodeposition of Co-B/SiC composite coatings: Characterization and evaluation of wear volume and hardness

A. Villa-Mondragón[1], A. Martínez-Hernández[1], F. Manríquez[1], Y. Meas[1], J.J. Pérez-Bueno[1], Francisco J. Rodríguez-Valadez[1], J.C. Ballesteros[2], J. Morales-Hernández[1], Alia Méndez-Albores[3] and G. Trejo[1,*]

[1] Centro de Investigación y Desarrollo Tecnológico en Electroquímica (CIDETEQ), Parque Tecnológico Sanfandila, C.P. 76703, Pedro Escobedo, Querétaro, México
[2] Universidad Politécnica de Lázaro Cárdenas (UPLC), Laboratorio de Sustentabilidad Energética, Avenida Galeanas S/N, Colonia Las 600 Casas, C. P. 60950, Lázaro Cárdenas, Michoacán, México.
[3] Science Institute-ICUAP Benemérita Universidad Autónoma de Puebla, Ciudad Universitaria Puebla, 72530 Puebla, México
* Correspondence: gtrejo@cideteq.mx (G. Trejo)

Abstract: In the present paper, Co-B/SiC composite coatings were obtained via electrodeposition from colloidal suspensions with different concentrations of SiC particles and subsequent heat treatments at 350 °C. The composition, morphology and structure of the Co-B/SiC composite coatings were analyzed using glow discharge spectrometry (GDS), scanning electron microscopy (SEM) coupled with energy-dispersive spectroscopy (EDS) and X-ray diffraction (XRD). Hardness and tribological properties were also studied. The results showed that an increase in the SiC concentration in the colloidal suspensions resulted in both an increase in the SiC content and a decrease in the B content in the obtained Co-B/SiC coatings. The Co-B/SiC coatings were adherent, glossy and soft and exhibited a homogeneous composition in all thicknesses. By contrast, an increase in the SiC particle content of the Co-B/SiC composite coating from 0 to 2.56 at.% SiC reduced the hardness of the film from 680 to 360 HV and decreased the wear volume values from 1180 to 23 μm^3 N^{-1} m^{-1}, respectively (that is, the wear resistance increased). Moreover, when the Co-B/SiC coatings with SiC content ranging from 0 to 2.56 at.% SiC were subjected to a heat treatment process, the obtained coating hardness values were in the range of 1200 to 1500 HV and the wear volume values were in the range of 382 to 19 μm^3 N^{-1} m^{-1}.

Keywords: Co-B/SiC composite coatings; electrodeposition; hard coatings; wear volume

1. Introduction

Surface degradation is one of the main damages experienced by the metallic parts of machinery exposed to high stress in hostile environments. The surface degradation of these components causes a deterioration in their mechanical properties, such as their wear resistance and hardness, which results in machinery malfunctions. For many decades, hard coatings such as cadmium (Cd), nickel (Ni) or chromium (Cr) have been widely used to protect metal components and tools against wear. Although Cd, Ni, and Cr coatings are excellent protective coatings with good performance and durability, the U.S. Environmental Protection Agency (EPA) lists these elements as priority pollutants, and they are considered to be among the 17 most toxic heavy metals [1]. For these reasons, alternative materials have been studied for many years. In this sense, composite coatings have recently been studied as an alternative to hard Cr coatings. Composite coatings are formed by two phases: the metal matrix as the main phase and as the second phase; micro or nanoparticles occluded

in the metal matrix [2, 3]. The insoluble micro o nano particles occluded in the metal matrix can be nitrides, oxides and carbides (Si_3N_4, SiO_2, Al_2O_3, TiO_2, SiC, WC, graphite) and its function is to increase the wear resistance and hardness of the coatings [4, 5, 6, 7, 8, 9]. These phenomena are mainly attributed to the hardening of the metal matrix by finely dispersed ceramic particles. Ogihara *et al.* [10] reported that composite films with Ni-B as the matrix material and SiC particles as the second phase exhibit hardness values of 845 HV without heat treatment and 1490 HV with heat treatment. Balaraju and Seshadri showed that, when the content of Si_3N_4 particles occluded in a Ni-P metal matrix is increased, the wear resistance of the Ni-P/Si_3N_4 coating increases substantially [11]. Min-Chieh *et al.* [9] reported that the addition of SiC particles to a Ni-P metal matrix reduces the residual stress of the deposits and therefore eliminates surface cracking. Also, several studies on Ni/SiC composite coatings have reported significant improvement in the wear resistance when SiC particles are added in the nickel matrix [12, 13]. In another study, the addition of B_4C particles to the matrix of the metallic Ni-P(9 %) alloy was found to increase the wear resistance of Ni-P(9 %)/B_4C composites [14].

Recently, nanocrystalline cobalt (Co) coatings and Co alloys have been identified as good candidates for replacing the hard coatings of Cr, Cd or Ni because of their similar or improved mechanical properties [15, 16]. Additionally, Co is not considered a heavy metal that negatively affects human health [17]. In a previous work [18], we reported the formation of Co-B hard coatings with hardness values between 760 and 800 HV (very similar to those of hard Cr), depending on the content of B in the coating.

The novelty of the present work, consists in the preparation of Co-B/SiC composite coatings by electrodeposition method due to the need of coatings with low friction and an improved wear resistance for its application in fabrication of machines, parts and metal structures exposed to high stress and severe erosion conditions. The aim was to elucidate the effect of incorporated SiC particles in the Co-B metal matrix on the wear volume, friction coefficient, and hardness. The effect of thermally treated Co-B/SiC composite coatings was also studied.

2. Materials and Methods

2.1. Stability measurements of SiC particles in suspension

The stability analysis of SiC particles suspended in the electrolytic baths containing the dispersant cetyltrimethylammonium bromide (CTAB) was carried out using colloidal suspension of composition S_0 (= 0.14 M $CoCl_2 \cdot 6H_2O$ + 2.8 M KCl + 0.32 M H_3BO_3 + 0.19 M Dimethylamine borane (DMAB) (DMAB was used as a boron source) + 27.4 mM CTAB) + x g L^{-1} SiC (x = 0.0, 0.15, 0.6, 2.5, 5.0, 10.0, 15.0) at pH 5.0. The solutions were prepared using distilled ultrafiltered water (18 MΩ cm resistivity) and analytical-grade reagents (Sigma-Aldrich). The average size of the SiC particles was 100 nm (SkySpring Nanomaterials, Inc.).

This study was carried out with a Turbiscan analyser (mod. Lab Expert, Formulation Co., France) and cylindrical glass vials with a sample height of 43 mm. The analysis of the obtained transmittance profiles vs. vial height was performed as described in Ref. [19]. The scanning of the transmittance (T) along the glass vial was performed at intervals of 5 min for 8 h. From the graph of the transmittance (T) profiles vs. vial height, the thickness of the clarifying layer (ΔH (mm) = H_{sup} - H_{inf}) was calculated (see Fig. 1). H_{inf} (mm) was obtained by arbitrarily fixing the T_f (fixed transmittance) value at 1% T (T_f = 1% T) and measuring the value of the distance in the vial where the intersection occurs between the T of the sweep (as a function of time) and the value of T_f. H_{sup}, the length of the sample in the glass vial, was equal to 43 mm. The difference between the two distances measured in the glass vial ($\Delta H = H_{sup} - H_{inf}$) is indicative of the precipitation of the SiC particles. High values of ΔH are indicative of an unstable suspension, whereas small values are indicative of a stable suspension.

2.2. Electrodeposition and characterization of the Co-B/SiC composites coatings

The Co-B/SiC composite coatings were electrodeposited from colloidal suspensions S_0 + x gL^{-1} SiC (x = 0.0, 0.15, 0.6, 2.5, 5.0, 10.0, 15.0) at pH 5.0 using a parallel-plate cell of 50-mL capacity and with an inter-electrode distance of 5 cm. AISI 1018 steel plates (2.5 × 5.5 cm^2 of exposed area) were used as the cathodes and graphite plates were used as the anodes. The coatings were deposited under galvanostatic conditions by applying 8.6 mA cm^{-2} for 56 min at 25 °C. The current density was selected from additional tests (not presented here) using a Hull cell for each of the electrolytic baths.

The deposited phases of the Co-B/SiC composite coatings were analyzed by X-ray diffraction (XRD) using a Bruker diffractometer (model D8 Advance) in the Bragg-Brentano arrangement with Cu Kα radiation (α = 1.54 Å). The 2θ range from 30° to 150° was recorded at a scan rate of 0.2° s^{-1}. The morphologies of the coatings were evaluated using scanning electron microscopy (SEM) (JEOL JSM-6510 LV) coupled to an energy-dispersive spectroscopy (EDS) analyser (Bruker Quantax 200). The elemental composition profiles of the Co-B/SiC composite coatings as a function of the thickness of the coatings were obtained using the glow discharge spectroscopy (GDS) technique (Horiba, model GD Profiler 2).

Hardness tests of the obtained Co-B/SiC composite coatings were carried out using an automatic hardness testing system (Matsuzawa, mod. MXT-ALFA) under an applied load of 25 g for 15 s. The final hardness values reported are the average of six measurements.

The wear volume tests were performed using a ball-on-disk tribometer (CSM instruments) in air at 25 °C and a relative humidity of approximately 39 % in dry conditions, without lubrication. Balls made of WC (6-mm diameter) (Anton-Paar) with a hardness of 3500 HV were used as the counter body in the wear tests. All wear volume tests were performed under a 2-N load at a sliding speed of 4.2 cm s^{-1}. The wear volume tests were performed in triplicate and in accordance with standard ASTM G99 [20]. During the tests, the sliding time and friction coefficient were automatically recorded.

3. Results and Discussion

3.1. Stability analyses of the system SiC particles/CTAB in colloidal suspensions

To uniformly occlude the SiC particles in the metallic matrix during the electrodeposition process of Co-B/SiC composite coatings, the SiC particles must be kept suspended in the electrolytic solution, which is achieved using a dispersant, preferably of the cationic type, i.e., CTAB. Therefore, before the electrodeposition of the Co-B/SiC composite coatings, the stability of the SiC particles in an electrolytic bath with CTAB as a dispersant was studied.

The stability of the SiC particles suspended in colloidal suspensions S_0 + x gL^{-1} SiC (x = 0.0, 0.15, 0.6, 2.5, 5.0, 10.0, 15.0) at pH 5.0 was analyzed at 25 °C using a dispersion-stability analyser. The analysis was based on the transmittance (T) profiles vs. the vial height obtained at different times. Typical transmittance profiles (obtained at different times) vs. the vial height of the SiC particles in a colloidal suspension are shown in Fig. 1. A small increase in ~ 5 % T is observed in the region from 0 to 1 mm (bottom of the vial); this behavior indicates the formation of a clarifying zone in this region. In the region from 1 to 42 mm, transmittance values close to zero (~0 % T) are observed during the 8 h of the experiment, indicating that the solution is opaque in this range because the SiC particles form a stable suspension. Finally, a small clarifying zone (ΔH) is formed in the range from 42.5 to 43 mm (top of the vial). Therefore, when CTAB was used as a dispersant, stable suspensions of SiC particles were obtained during a period of 8 h.

Preprints (www.preprints.org) | NOT PEER-REVIEWED | Posted: 4 April 2019 doi:10.20944/preprints201904.0056.v1

Peer-reviewed version available at Coatings 2019, 9, 279; doi:10.3390/coatings9040279

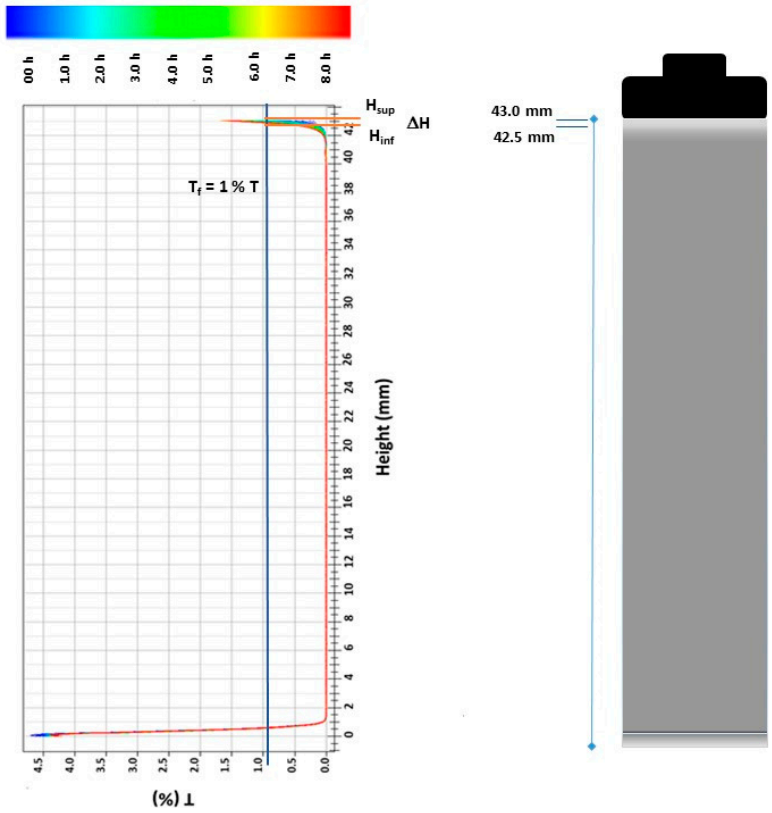

Figure 1. a) Transmittance profiles of the colloidal suspension S_0 (= 0.14 M $CoCl_2 \cdot 6H_2O$ + 2.8 M KCl + 0.32 M H_3BO_3 + 0.19 M DMAB + 27.4 mM CTAB) with 10 g L^{-1} SiC. Data are reported as a function of time (0 to 8 h) and sample height (0 to 43 mm). b) Schematic representation of the dispersion of SiC particles in the S_0 solution with 10 g L^{-1} SiC.

Fig. 2 shows the thickness variation of the clarifying layer (ΔH) in the colloidal suspensions as a function of time for different concentrations of SiC particles. An increase in the concentration of SiC particles in the colloidal suspensions causes a significant decrease in the values of the thickness variation of the clarifying layer (ΔH) as a function of time. Lower values of ΔH were obtained for the highest concentrations of SiC particles (15 and 10 gL^{-1}). After 8 h of experimentation, the ΔH value of the aqueous suspensions with both 15 and 10 gL^{-1} SiC was only 0.5 mm, whereas for the suspension with 0.15 gL^{-1} SiC, ΔH was 37 mm in the same period of time.

The greater stability of the SiC particles in the colloidal suspensions is associated with the adsorption of CTAB molecules on their surface. Due to its hydrophilic functional groups and its spatial structure, the adsorbed CTAB increases the steric hindrance and electrostatic repulsion among the SiC particles [21].

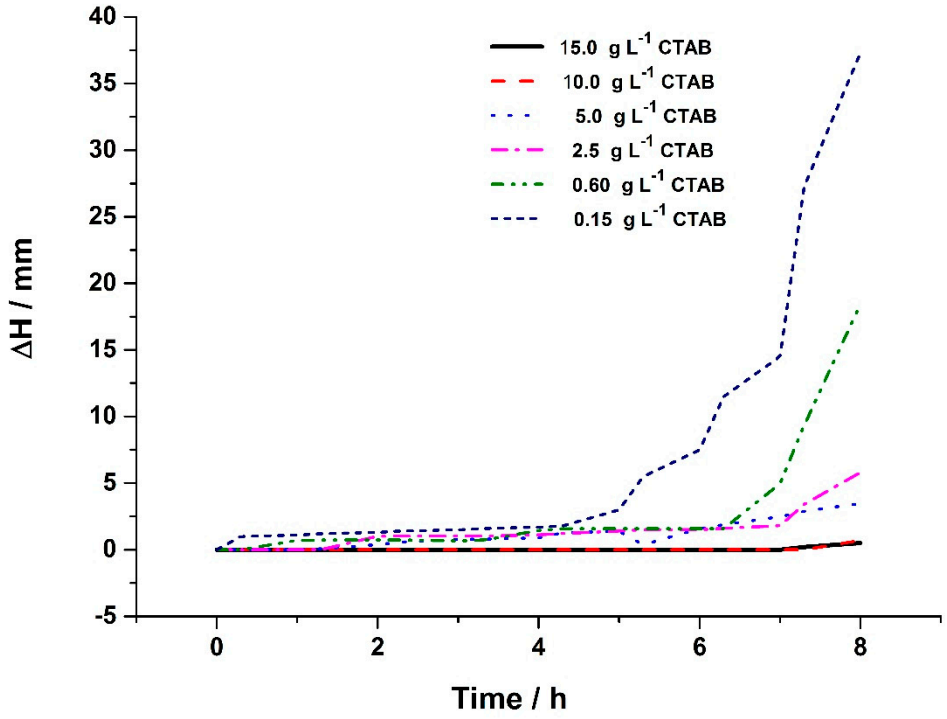

Figure 2. Effect of the SiC concentration in the colloidal suspensions on the clarifying layer thickness (ΔH) as a function of time (0 to 8 h).

3.2. Co-B/SiC composite coating composition

The Co-B/SiC composite coatings were electrodeposited under galvanostatic conditions (8.6 mA cm^{-2} for 56 min) from colloidal suspensions S_0 + x gL^{-1} SiCP (x = 0.0, 0.15, 0.60, 2.5, 5.0, 10.0, 15.0) at a pH = 5.0. The thickness of the coatings was 7.3 ± 1.3 µm, which was measured by X-ray fluorescence.

GDS was used to analyse the influence of the SiC particle concentration in the colloidal suspensions on the distribution and relative concentration of the elements Co, B and Si in the obtained Co-B/SiC composite coatings. For this analysis, we assumed that the detected Si signal corresponds to SiC. Moreover, coating analysis was stopped once the substrate signal (Fe) was constant and close to 100 at.%. Fig. 3 shows GDS profiles of the atomic percentage (at.%) variation of Co, B, Si, O and C as a function of depth of a Co-B/SiC composite coating obtained from a colloidal suspension S_0 + 2.5 g L^{-1} SiC. In Fig. 3, to better observe the behavior of the elements, the signal corresponding to B was amplified by a factor of 5 and the signal corresponding to Si was amplified by a factor of 10. On the surface of the coating, the formation of a surface oxide film of approximately 0.45 µm in thickness was observed. After the surface oxide layer was removed, the signals of C (~5.0 at.%), O (~7.0 at.%), Si (~1.7 at.%), Co (~ 75.0 at.%) and B (~ 7.0 at.%) were detected. These signals are practically constant throughout the thickness of the Co-B/SiC coating (approximately 7 µm). Subsequently, they decrease rapidly, while the substrate signal (Fe) increases, forming an interface zone between the substrate (Fe) and the Co-B/SiC coating. At depths greater than 8 µm, the substrate signal (Fe) remains constant and close to 100 at.%. In addition, the behaviors of the signals corresponding to Si, C, and B are similar to that of the Co signal. This behavior demonstrates the simultaneous co-position of Co, B, and Si. Moreover, Fig. 3 clearly shows the homogeneous distribution of all the elements inside the coating. A similar behavior was observed for all of the investigated SiC concentrations.

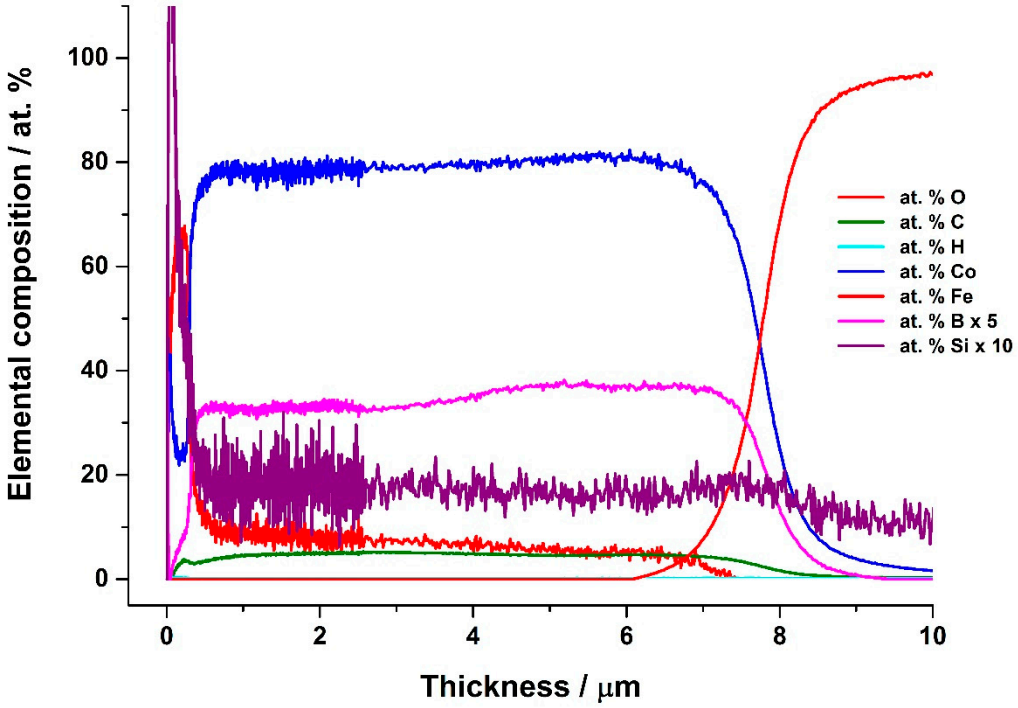

178

179 **Figure 3.** GDS elemental-distribution profiles of a Co-B/SiC composite coating electrodeposited from
180 colloidal suspension S_0 (= 0.14 M $CoCl_2 \cdot 6H_2O$ + 2.8 M KCl + 0.32 M H_3BO_3 + 0.19 M DMAB + 27.4 mM
181 CTAB) with 10 g L^{-1} SiC.

182 From the GDS analyses of the obtained coatings, Fig. 4 shows the variation in the content of B
183 (at.%) and Si (at.%) in the Co-B/SiC composite coatings as a function of the SiC particle concentration
184 in the colloidal suspensions. This figure shows that the Si content in the coating increases and reaches
185 a saturation point of 2.5 ± 0.06 at.% Si when the concentration of SiC in the electrolytic bath was
186 greater than or equal to 5 g L^{-1}. In contrast, the content of B in the coating decreases as the
187 concentration of SiC in the electrolytic bath increases. At concentrations greater than or equal to 10 g
188 L^{-1}, the B content remains constant at 1.5 ± 0.08 at.%. An equivalent behavior for the variation in P
189 during the electrodeposition of the Ni-P-SiC composite has been observed by other authors [9, 22,
190 23].

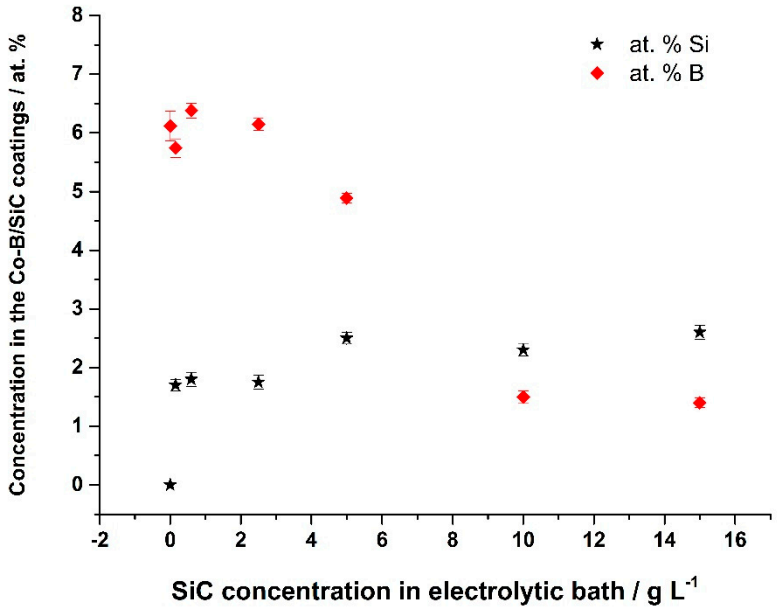

Figure 4. Changes in the B (at.%) and Si (at.%) contents in the Co-B/SiC composite coatings according to the concentration of SiC in the colloidal suspensions.

3.3. Co-B/SiC composite coating morphology

Fig. 5 shows SEM images of the Co-B/SiC composite coatings obtained from colloidal suspensions containing different concentrations of SiC (i.e., coatings with different at.% SiC). In the absence of SiC in the electrolytic bath (Fig. 5a) (0 at.% SiC in the coating), a compact, smooth, adherent, and shiny Co-B coating is formed. Additionally, the surface of the coating shows superficial microfissures, likely due to the inner coating stress. The inset of Fig. 5a shows the amorphous structure of the Co-B coating. Furthermore, occlusion of SiC particles in the metal matrix causes a change in morphology towards an amorphous-crystalline structure of the Co-B/SiC composite coatings obtained (see Fig. 5b (1.76 at.% SiC), Fig. 5c (2.56 at.% SiC)). Semi-spherical structures of nanometric size were formed on top of the clusters. In addition, by increasing the content of SiC particles in the coatings, the size of the surface micro-fissures decreased, which is indicative of a lower level of internal stress inside the coatings. This behavior is associated with the inhibition of the hydrogen evolution reaction, due to the adsorption of the CTAB dispersant on the surface of the substrate.

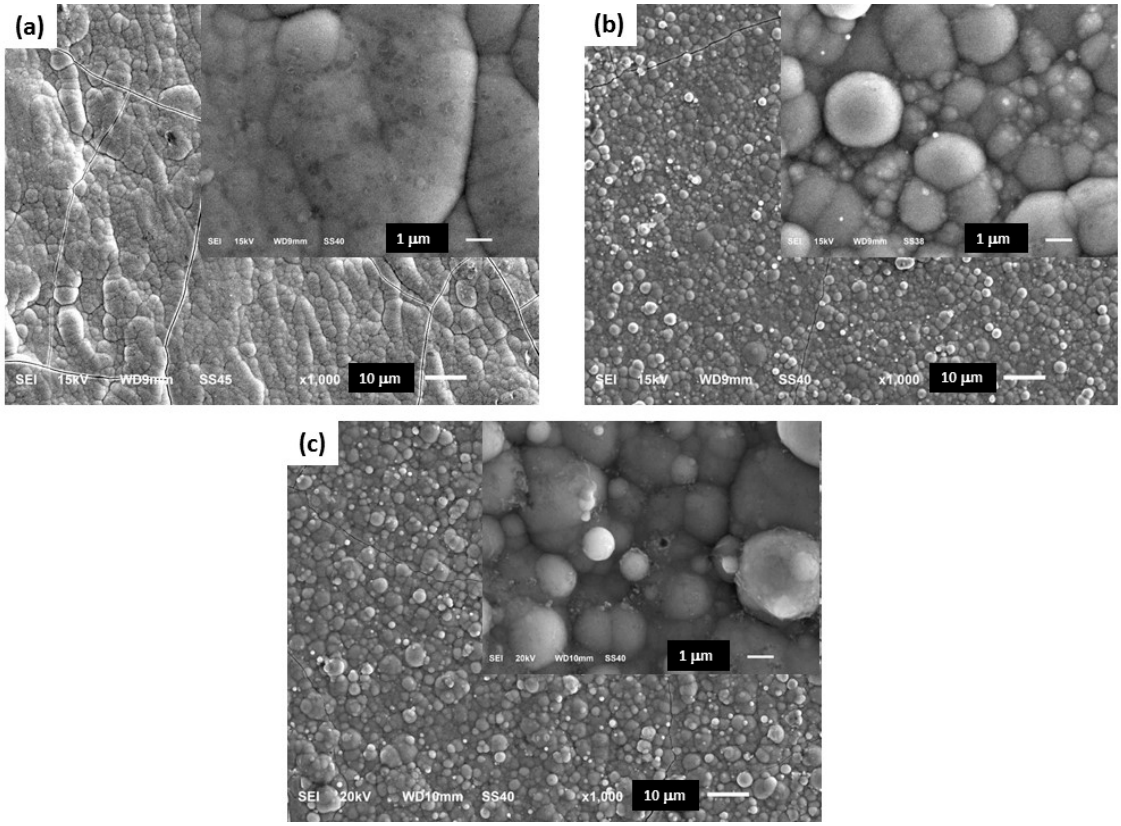

Figure 5. a) SEM images of the Co-B coatings obtained from colloidal suspension S_0 (= 0.14 M $CoCl_2 \cdot 6H_2O$ + 2.8 M KCl + 0.32 M H_3BO_3 + 0.19 M DMAB + 27.4 mM CTAB); b) SEM images of the Co-B/SiC composite coatings obtained from the colloidal suspension S_0 + 2.5 g L^{-1} SiC; and c) SEM images of the Co-B/SiC composite coatings obtained from the colloidal suspension S_0 + 15 g L^{-1} SiC.

The elemental mapping analysis obtained from the surface of the Co-B/SiC (2.56 at.% SiC) coating (Fig. 6) showed that the SiC particles were homogeneously distributed on the surface of the coating. These results, together with the GDS results shown in the previous section, confirm the homogeneous occlusion of the SiC particles in the Co-B coating matrix; the same behavior was observed for all concentrations of SiC particles studied. This behavior is the result of improving the migration of the SiC particles towards the negatively charged electrode surface (cathode), due to the increase in the positive electric charge of the SiC particles that occurs because of the adsorption of the cationic dispersant CTAB on the surface of the SiC particles [24].

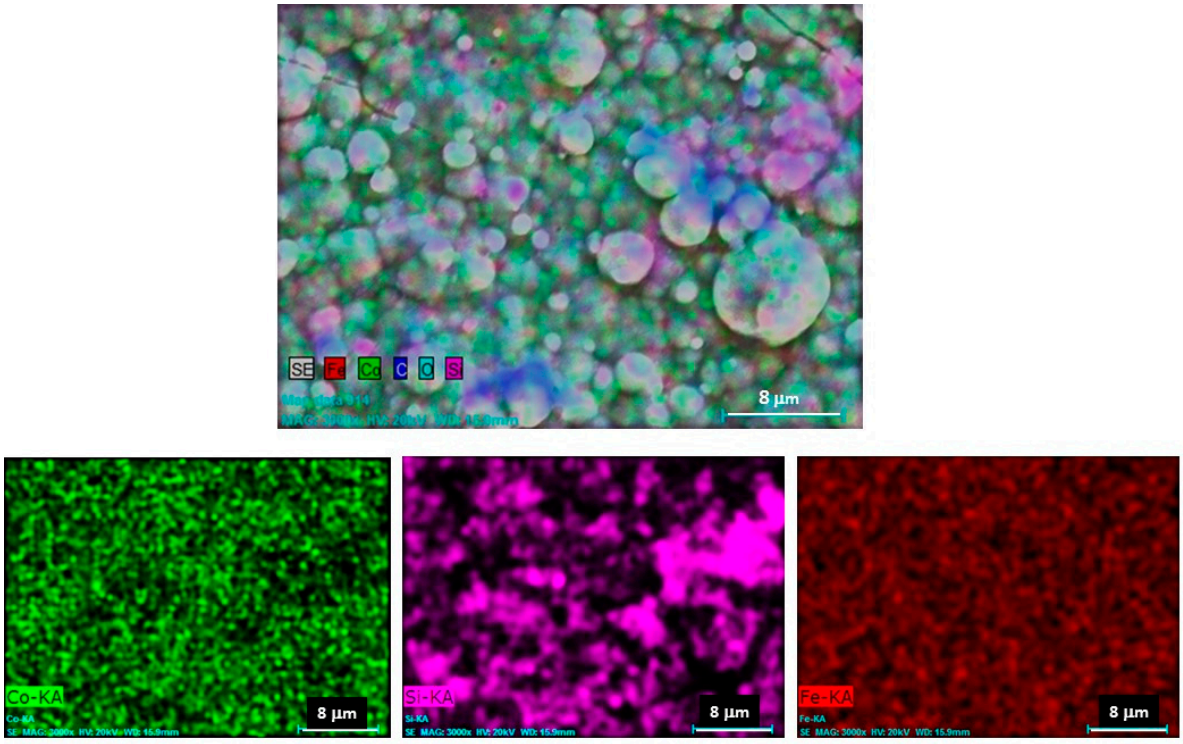

Figure 6. Elemental mapping profile of a Co-B/SiC composite coating obtained from a colloidal suspension S_0 with 10 g L^{-1} SiC.

3.4. XRD Analysis

The structural changes of the Co-B/SiC composite coatings were characterized by XRD. Fig. 7 shows the corresponding XRD diffractograms. For the Co-B (0 at.% SiC) coating, the XRD diffractogram shows a broad peak at $2\theta = 44.44°$, which is characteristic of an amorphous Co-B structure. This behavior is altered when the Co-B/SiC composite is formed by the occlusion of SiC particles into the Co-B alloy. When the amount of SiC particles in the Co-B matrix was increased, the crystallinity of the Co-B/SiC composite increased. These results corroborate the behavior observed in the SEM micrographs in Figs. 5a-c. Bozzini *et al.* observed a similar phenomenon during the occlusion of B_4C particles in the matrix of Ni-P alloy; this behavior was tentatively explained by the particles promoting crystallization at low temperatures by providing nucleation sites for the precipitation of nuclei in the amorphous matrix [14, 25, 26].

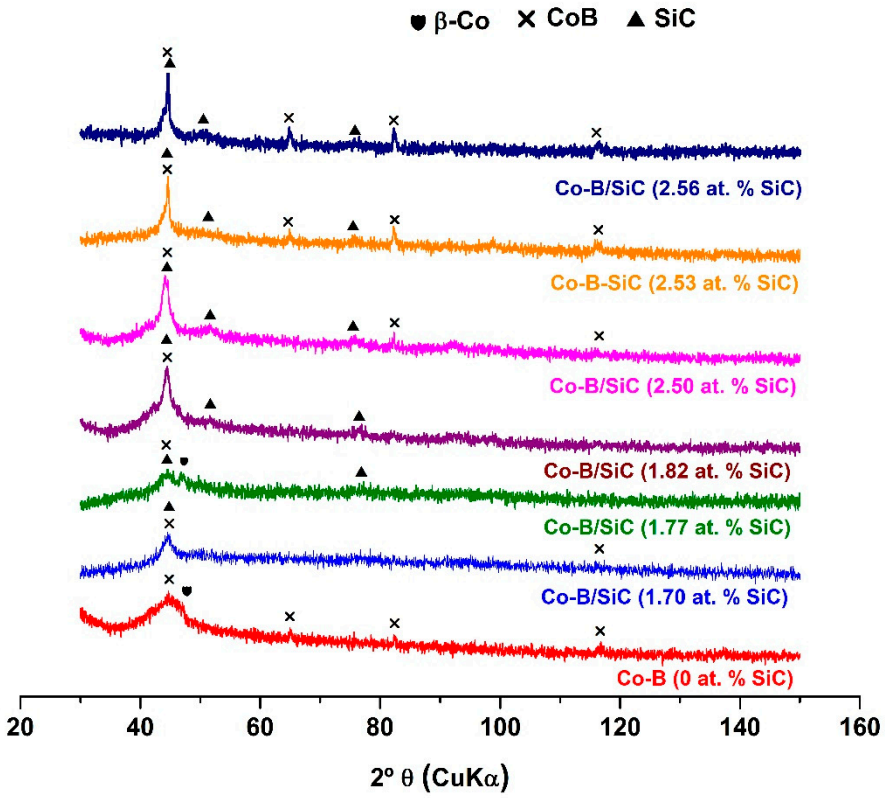

Figure 7. Normalized XRD patterns of Co-B/SiC composite coatings with different SiC contents (at.%) obtained under galvanostatic conditions (8.6 mA cm^{-2} for 56 min). βCo (JCPDS 01-089-4308), CoB (JCPDS 01-089-4308), SiC (JCPDS 00-042-1360).

3.5. Microhardness of the Co-B/SiC composite coatings

Fig. 8 shows the behavior of the microhardness of the Co-B/SiC composite coatings produced as a function of the content of SiC particles in the coating. The microhardness of the Co-B/SiC coatings decreases with increasing SiC content in the Co-B/SiC composite. This behavior can be associated with a decrease in the content of B by increasing the content of SiC particles in the coating (see Fig. 4). In previous studies, the hardness of Co-B coatings was found to increase with increasing B content in the coating due to the formation of the hard intermetallic compound Co-B [18, 27]. In the present study, the results in Fig. 4 show that increasing the content of SiC particles in the colloidal suspensions increases the content of SiC particles and reduces the B content in the coating. Thus, the observed decrease in microhardness can be caused by the decrease in the B content in the coating.

Preprints (www.preprints.org) | NOT PEER-REVIEWED | Posted: 4 April 2019 doi:10.20944/preprints201904.0056.v1

Peer-reviewed version available at Coatings 2019, 9, 279; doi:10.3390/coatings9040279

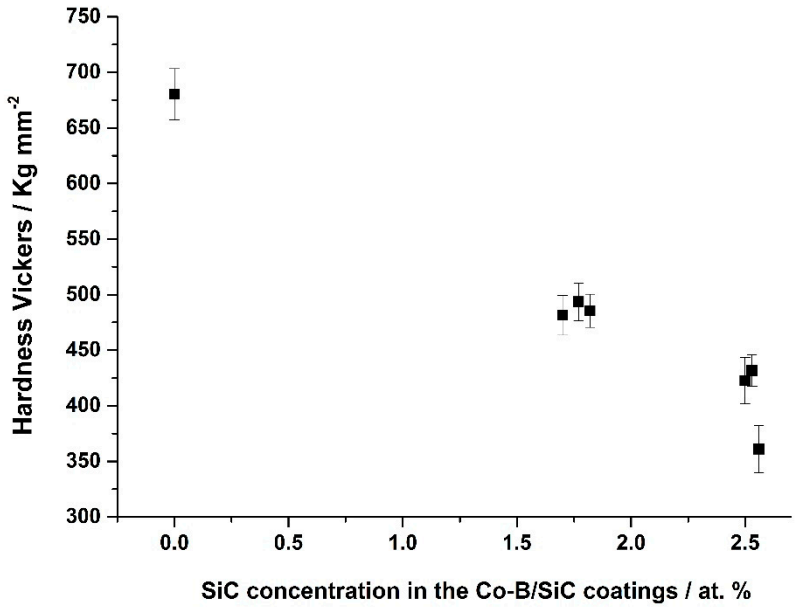

Figure 8. Variation in Co-B/SiC composite coating hardness as a function of the SiC content in the coatings.

3.6. Tribological behavior

Table 1 shows the average values of the wear volume measured at the end of the test (300 m sliding distance) as a function of the amount of SiC particles in the obtained Co-B/SiC coatings. The wear volume decreased (i.e., the wear resistance increased) by increasing the content of SiC in the coatings. The lowest wear volume value (23.0 $\mu m^3/Nm$) was obtained for Co-B/SiC (2.5 at.% SiC) coating; this value is lower than that reported for different systems, such as Ni-P-FGD composite [28], Ni-B [29], NiP/SiC [30], Ni-P(9 %)/B4C [14], Co-P [15] or Co-B [18] and is similar to that of a hard Cr coating [28].

Table 1. The relationship between the SiC content in the Co-B/SiC composite coatings and the wear volume and friction coefficients of the Co-B/SiC coatings deposited under galvanostatic conditions (8.6 mA cm^{-2} for 56 min).

SiC concentration in the colloidal suspensions (gL^{-1})	SiC in the coatings (at.%)	Wear volumen loss (x 10^{-7} mm^3 $N^{-1}m^{-1}$)	Friction Coefficient (μ)
0	0	11.80 ± 0.13	0.444 ± 0.03
0.15	1.70	3.49 ± 0.19	0.417 ± 0.008
0.60	1.77	2.83 ± 0.21	0.353 ± 0.012
2.50	1.82	0.46 ± 0.12	0.304 ± 0.008
5.00	2.50	0.23 ± 0.08	0.312 ± 0.010
10.00	2.54	0.23 ± 0.10	0.313 ± 0.010
15.00	2.56	0.27 ± 0.11	0.312 ± 0.082

To understand the wear mechanism of the coatings, we analyzed the worn surface of the Co-B/SiC composite coatings with different SiC content by SEM. In the Co-B coatings (Fig. 9a), the presence of torn patches and some detachment within the worn tracks is typical evidence of that a plastic deformation was carried out in this process, which is indicating that the principal mechanism is adhesive wear. The results show that increasing SiC particles content up to 2.5 at.% SiC (Fig. 9b) it is possible to observe the formation of the thinner grooves on the worn surface. This behavior is an evidence of beneficial effect of the incorporation of SiC, which improved wear resistance and low friction. A similar behavior was observed in the wear tests of the Co-B/SiC composite coatings. Compared with the other Co-B/SiC coatings, the Co-B/SiC coating with 2.5 at.% SiC (Fig. 9b) exhibited the narrowest width and shallowest plough lines. These findings indicated that this coating exhibited the best wear resistance.

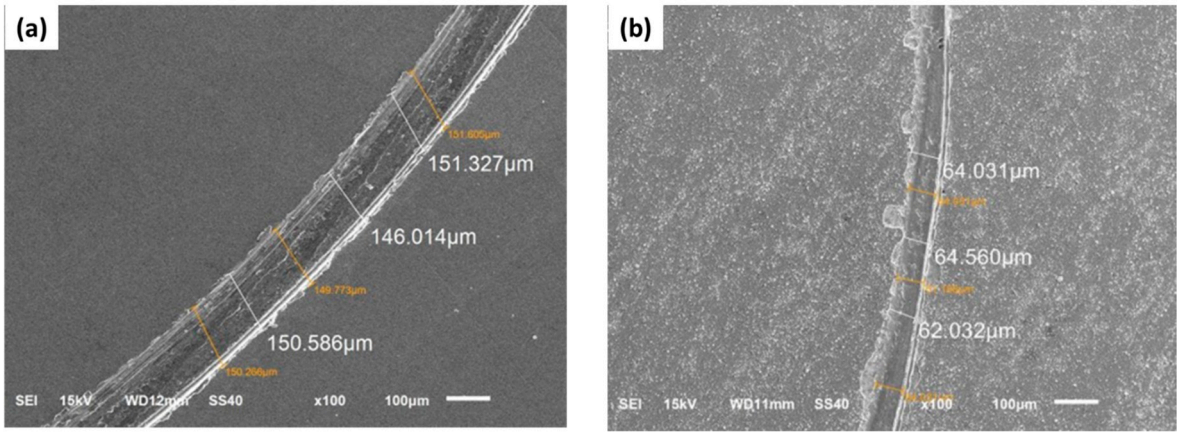

Figure 9. Typical SEM micrographs of the wear track pattern of coatings in their as-deposited condition: a) Co-B coating and b) Co-B/SiC (2.5 at.% SiC) composite coating.

Likewise, the average values of the coefficients of friction (μ) of Co-B/SiC coatings, which were obtained simultaneously during the wear test, decreased with increasing SiC content in the coating and reached a constant value of approximately 0.31 at the highest concentrations of SiC. The obtained coefficient-of-friction values are lower than those reported for systems such as Ni-P/SiC [30,23,12], Ni-B [31], Ni-B-diamond [32], Ni-P/B_4C [14], and Ni-SiC [33] but are higher than those reported for Ni-P-GDF and hard Cr coatings [19]. The above results imply that the SiC particles occluded in the coating matrix, act as a lubricant, since by increasing the content of SiC particles in the Co-B/SiC coatings, these increase the lubricating properties of the coatings.

3.7. Effect of heat treatment on the hardness, wear volume and coefficients of friction (μ)

The effect of a 1-h heat treatment at 350 °C in an air atmosphere on the hardness, wear volume and coefficient friction of the Co-B/SiC composite coatings was studied.

The microhardness results are shown in Fig. 10. As expected, the hardness of the coatings increased considerably after they were thermally treated; hardness values from 1200 to 1500 HV were obtained over the entire range of SiC concentrations (0 to 2.56 at.% SiC, respectively). Thus, the presence of SiC particles in the coatings has little influence on their hardness.

Preprints (www.preprints.org) | NOT PEER-REVIEWED | Posted: 4 April 2019 doi:10.20944/preprints201904.0056.v1

Peer-reviewed version available at Coatings 2019, 9, 279; doi:10.3390/coatings9040279

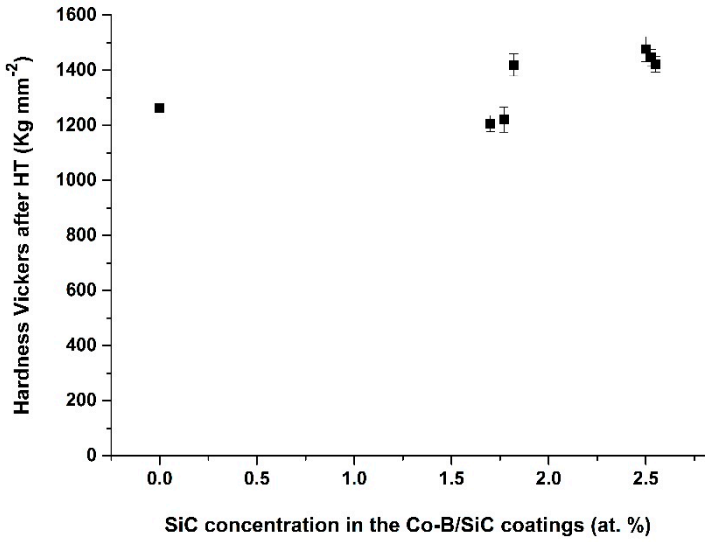

Figure 10. Variation in the Co-B/SiC composite coating hardness as a function of the SiC content in the coatings after heat treatment at 350 °C for 1 h.

Therefore, the increase in hardness is mainly associated with the crystallization of the hard intermetallic species Co_3B, which occurs between 200 and 400 °C, which is further confirmed by XRD patterns (Fig. 11). In Fig. 11, the XRD patterns show that when the Co-B/SiC (2.56 at.% SiC) coating was thermally treated at 350 °C, the structure became crystalline and peaks corresponding to crystalline Co_3B and Co_3O_4 appeared. A similar behavior was obtained in all Co-B/SiC coatings analyzed.

The GDS analysis performed on the Co-B/SiC (2.56 at.% SiC) composite coating after being heat treated at 350 °C, presented the following composition: 2.13 ± 0.3 at.% SiC, 1.66 ± 0.13 at.% B, 0.7 ± 0.2 at.% O.

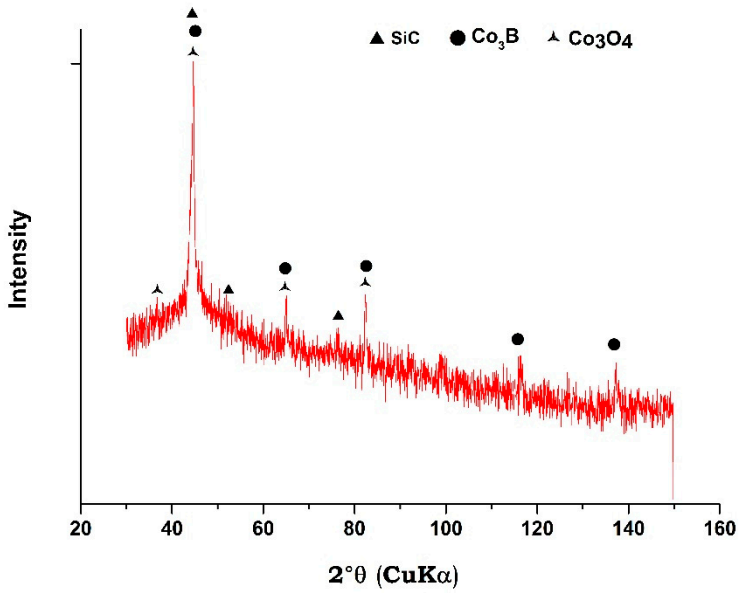

Figure 11. Normalized XRD pattern of the Co-B/SiC (2.56 at.% SiC) composite coating after heat treatment at 350 °C. SiC (JCPDS 00-042-1360), Co_3B (JCPDS 03-065-2414), Co_3O_4 (JCPDS 00-043-1003).

Table 2 shows the values of wear volume and friction coefficient obtained for Co-B/SiC coatings with different SiC contents and heat treatment at 350 °C. Both values decrease with increasing SiC content in the coating. Additionally, the values obtained are similar to those obtained for Co-B/SiC coatings without heat treatment (see Table 1). Therefore, the heat treatment strongly influences the hardness of the coatings due to the formation of the Co_3B intermetallic species but has little influence on the volume of wear and the coefficient of friction, which are mainly decreased by the incorporation of the SiC particles into the metal matrix.

Table 2. The relationship between the SiC content in the Co-B/SiC composite coatings and the wear volume and friction coefficients of the Co-B/SiC coatings deposited under galvanostatic conditions (8.6 mA cm^{-2} for 56 min). Values obtained after thermal treatment the coatings at 350 °C for 1 h.

SiC concentration in the colloidal suspensions (gL^{-1})	SiC in the coatings at.%	Wear volume loss after HT ($\times 10^{-7}$ mm^3 $N^{-1}m^{-1}$)	Friction Coefficient After HT (μ)
0	0	3.82 ± 0.09	0.260 ± 0.03
0.15	1.70	2.72 ± 0.11	0.255 ± 0.01
0.60	1.77	1.32 ± 0.08	0.245 ± 0.03
2.50	1.82	0.93 ± 0.10	0.238 ± 0.03
5.00	2.50	0.44 ± 0.08	0.213 ± 0.08
10.00	2.54	0.35 ± 0.10	0.215 ± 0.02
15.00	2.56	0.19 ± 0.07	0.208 ± 0.01

4. Conclusions

The objective of this work was to obtain Co-B/SiC composite coatings with different contents of occluded SiC particles via electrodeposition. The composition, hardness, wear volume (wear resistance) and coefficient of friction of the coatings before and after heat treatment at 350 °C for 1 h were analyzed. The results showed that Co-B/SiC composite coatings of homogeneous composition were obtained by electrodeposition using CTAB as a dispersant in a colloidal suspension. When studying the influence of the concentration of SiC particles in the colloidal suspensions on the composition of the obtained Co-B/SiC coatings, we found that the amount of occluded SiC particles in the coatings increased and the content of B decreased with increasing concentration of SiC particles in the colloidal suspensions. The variation in the composition of the coatings substantially affected their physical characteristics. Co-B/SiC coatings with a higher B content and a lower SiC particle content presented a higher hardness and lower wear resistance, whereas coatings with a lower B content and a higher SiC particle content exhibited a lower hardness and greater wear resistance. Therefore, the occlusion of SiC particles in the metal matrix increases the wear resistance of the coatings.

The heat treatment at 350 °C for 1 h had little influence on the wear volume or coefficient of friction of the Co-B/SiC coatings because the values obtained after the heat treatment were similar to those obtained without the heat treatment. However, the hardness of the coatings increased considerably from 1400 to 1500 HV for Co-B/SiC coatings with a SiC particle content in the range of 0 to 2.56 at.%, respectively. This behavior was attributed to the formation of the hard intermetallic compound Co_3B.

From the obtained results, it is possible to propose the Co-B/SiC composites coatings can be applied for the protection of steel parts against wear. Also, it is possible to propose that the coatings obtained in this work are an excellent alternative to replace to the coatings of Cr.

Author Contributions: Formal analysis, F. Manríquez and J.J. Pérez-Bueno; Investigation, Francisco J. Rodríguez-Valadez and J. Morales-Hernández; Methodology, A. Villa-Mondragón and A. Martínez-Hernández; Validation, Y. Meas and J.C. Ballesteros; Writing – review & editing, Alia Méndez-Albores and G. Trejo.

Funding: This research was funded by CONACyT, projects: PN/2015-01-248, Sectorial Fund CONACyT-SENER (project 259334) Energy Sustainability and CONACyT-SENER (project 248090, cluster de bioturbosine), Sustentabilidad Energética 2104-05. A. Villa-Mondragón is grateful to CONACyT for scholarship support.

Conflicts of Interest: The authors declare no conflict of interest

References

1. Eskin, S.; Berkh, O.; Rogalsky, G.; Zahavi. J. Co-W Alloys for Replacement of Conventional Hard Chromium. *Plat. Surf. Finish.* **1998**, 85, 79-83.
2. Hovestad A., Janssen L.J.J., Electrochemical codeposition of inert particles in a metallic matrix, J. Appl. Electrochem. **1995**, 25, 519-527.
3. Wang W., Hou F-Y, Wang H. Guo H-T., Fabrication and Characterization of Ni-ZrO2 composite nano-coatings by pulse electrodeposition. Scripta Materialia **2005**, 53, 613-618.
4. Shahri Z., Allahkaram S.R., Effect of plating parameters on microstructure and tribological properties of Co-B(hexagonal) nano composite coatings. Trans. Nonferrous Met. Soc. China. **2013**, 23, 2929-2938.
5. Venkataraman B., Sundararajan G., The sliding wear behavior of Al-SiC particulate composites-I. Macrobehavior. Acta Mater. 1996, 44, 451-460.
6. Ortiz-Merino J.L., Todd R.I., Relationship between wear rate, surface pullout and microstructure during abrasive wear of alumina and alumina/SiC nanocomposites. Acta materialia 2005, 53, 3345-3357.
7. Sanchez Egea A.J., Martynenko V., Abate G, Deferrari N., Martínez Krahmer D., López de Lacalle L.N. Friction capabilities of graphite-based lubricants at room and over 1400 K temperaturas. Int. J. Adv. Manuf. Technol., 2019. doi.org/10.1007/s00170-019-03290-4.
8. Hong-Kee, L.; Ho-Young, L.; Jun-Mi, J. Electrolytic deposition behaviors of Ni-SiC composite coatings containing submicron-sized SiC particles. *Met. Mater. -Int.* **2008**, 14, 599-605.
9. Min-Chieh, Ch.; Ming-Der, G.; Shih-Tsung, K.; Ya-Ru, H.; Shinn-Tyan, W. The Ni–P–SiC composite produced by electro-codeposition. *Mater. Chem. Phys.* **2005**, 92, 146-151.
10. Ogihara, H.; Wang, H.; Saji, T. Electrodeposition of Ni-B/SiC composite films with high hardness and wear resistance. *Appl. Surf. Sci.* **2014**, 296, 108-113.
11. Balaraju, J.N.; Seshadri, S.K. Synthesis and corrosion behavior of electroless Ni-P-Si_3N_4 composite coatings. *J. Materials. Sci. Lett.* **1998**, 17, 1297-1299.
12. Aslayan, I.R.; Bonino, J.-P.; Celis, J.-P. Effect of submicron SiC particles on the wear of electrolytic NiP coatings Part 1. Uni-directional sliding. *Surf. Coat. Tech.* **2006**, 200, 2909-2916.
13. Garcia I., Fransaer J., Celis J.-P., Electrodeposition and sliding wear resistance of nickel composite coatings containing micron and submicron SiC particles. Surf. Coat. Technol. 2001, 148, 171-178.
14. Bozzini, B.; Martini, C.; Cavalloti, P.L.; Lanzoni, E. Relationships among crystallographic structure, mechanical properties and tribological behavior of electroless Ni-P(9%)/B_4C. *Wear* **1999**, 225-229, 806-813.
15. Prado, R.A.; Facchini, D.; Mahalanobis, N.; Gonzalez, F.; Palumbo, G. Electrodeposition of nanocrystalline cobalt alloy coatings as a hard chrome alternative. In: DoD Corrosion Conference, Gaylord National, Washington DC 2009. USA, August 10-14, 2009.
16. Friedman H., Eidelman O., Feldman Y., Moshkovich A., Perfiliev V., Rapoport I., Cohen H., Yoffe A., Tenne R. Fabrication of self-lubricanting cobalt coatings on metal surface. Nanotechnology. 2007, 18, 115703-115710.
17. Duruibe, J.O.; Ogwuegbu, M.O.C.; Egwurugwu, J.N. Heavy metal pollution and human biotoxic effects. *Int. J. Phys. Sci.* **2007**, 2, 112-118.
18. Martínez-Hernández, A.; Meas, Y.; Pérez-Bueno, J.J.; Ortíz-Frade, L.A.; Flores-Segura, J.C.; Méndez-Albores, Alia; Trejo, G. Electrodeposition of Co-B hard coatings: characterization and tribological properties. *Int. J. Electrochem. Sci.* **2017**, 12, 1863-1873.
19. Méndez-Albores, A.; González-Arellano, S.G.; Reyes-Vidal, Y.; Torres, J.; Talu, S.; Cercado, B.; Trejo G. Electrodeposited chrome/silver nanoparticle (Cr/AgNPs) composite coatings: Characterization and antibacterial activity, *J. Alloys Comp.* **2017**, 710, 302-311.
20. Fazio, P.C. *et al.*, editors. Annual Book of ASTM Standards, Wear and Erosion; Metal Corrosion. ASTM G99-05. Standard Test Method for Wear Testing with a Pin-on-Disk Apparatus. Philadelphia: ASTM 2010.
21. Cerruti, B.; de Souza, C.; Castellan, A.; Ruggiero, R.; Frollini, E. Carboxymethyl lignin as stabilizing agent in aqueous ceramic suspensions. *Ind. Crops. Prod.* **2012**, 36, 108-115.
22. Malfati, C.F.; Ferreira, J.Z.; Oliveira, C.T.; Rieder, E.S.; Bonino, J.P. Electrochemical behavior of Ni-P/SiC composite coatings: Effect of heat treatment and SiC particle incorporation. *Materials and Corrosion* **2012**, 63, 36-43.
23. King_Hsu, H.; Wen-Hwa, H.; Shit-Tsung, K.; Ming-Der, G. Ni-P/SiC composite produced by pulse and direct current plating. *Mater. Chem. Phys.* **2006**, 100, 54-59.

24. González-Arellano, S. G.; Avilés-Arellano, Luz Ma. R.; Manríquez, J.; Torres, J.; Ortega, R.; Meas, Y.; Trejo, G.; Méndez-Albores, A. Study of the Stability of Silver Particles Suspended using Cetylpyridinium Bromide (CPB) as Surfactant. *Chem. Sci. Rev. Lett.* **2015**, 4, 809-816.
25. Bozzini, B.; Cavallotti, P.L.; Parisi, G. Corrosion and erosion of electrodeposited Ni-P/B4C composites. *Brit. Corros. J.* **2001**, 36, 49-55.
26. Bozzini, B.; Lecis, N.; Cavallotti, P.L. Structure and Magnetic properties of nanocrystalline Ni-P prepared by autocatalytic chemical deposition. *J. Phys IV France* **1998**, 8, 371-374.
27. Lim, T.; Kim, J.J. Effect of B and W contents on hardness of electroless Co alloys thin films. *Korean Chem. Eng. Res.* **2018**, 56, 895-900.
28. Liping. W.; Yan, G.; Tao, X.; Qunji, X. Corrosion resistance and lubricated sliding wear behavior of novel Ni-P graded alloy as alternative to hard Cr deposits. *Appl. Surf. Sci.* **2006**, 252, 7361-7372.
29. Lee, K.H.; Chang, D. S.; Know, C. Properties of electrodeposited nanocrystalline Ni-B alloys films. *Electrochim. Acta* **2005**, 50, 4538-4543.
30. Aslanyan, I.R.; Bonino, J.-P.; Celis, J.-P. Effect of reinforcing submicron SiC particles on the wear of electrolytic NiP Coatings, Part 2: Bi-directional Sliding, *Surf. Coat. Tech.* **2006**, 201, 581-589.
31. Krishnaveni, K.; Sankara Narayanan, T.S.N.; Seshadri, S.K. Electrodeposited Ni-B coatings: Formation and evaluation of hardness and wear resistance. *Mater. Chem. Phys.* **2006**, 99, 300-308.
32. Monteiro, O.R.; Murugesan, S.; Khabashesku, V. Electrodeposited Ni-B and Ni-B metal matrix diamond nanocomposite coatings. *Surf. Coat. Tech.* **2015**, 272, 291-297.
33. Benea, L.; Bonora, P.L.; Berello, A.; Martelli, S. Wear corrosion properties of nanostructured SiC nickel composite coatings obtained by electroplating. *Wear* **2002**, 249, 995-1003.